

This discussion paper is/has been under review for the journal Climate of the Past (CP).
Please refer to the corresponding final paper in CP if available.

Constraints on ocean circulation at the Paleocene–Eocene Thermal Maximum from neodymium isotopes

A. N. Abbott¹, B. A. Haley^{1,2}, A. K. Tripathi³, and M. Frank²

¹CEOAS, OSU, 104 Ocean Admin. Bldg., Corvallis, OR 97331, USA

²GEOMAR Helmholtz Centre for Ocean Research Kiel, Wischhofstrasse 1–3, 24148 Kiel, Germany

³Department of Earth and Space Sciences, Department of Atmospheric and Oceanic Sciences, and Institute of the Environment and Sustainability, University of California, Los Angeles, CA 90095, USA

Received: 05 May 2015 – Accepted: 01 June 2015 – Published: 30 June 2015

Correspondence to: B. A. Haley (bhaley@coas.oregonstate.edu)

Published by Copernicus Publications on behalf of the European Geosciences Union.

Constraints on ocean circulation at the Paleocene–Eocene Thermal Maximum

A. N. Abbott et al.

Title Page

Abstract

Introduction

Conclusions

References

Tables

Figures



Back

Close

Full Screen / Esc

Printer-friendly Version

Interactive Discussion



Abstract

Global warming during the Paleocene Eocene Thermal Maximum (PETM) ~ 55 million years ago (Ma) coincided with a massive release of carbon to the ocean–atmosphere system, as indicated by carbon isotopic data. Previous studies have argued for a role for changing ocean circulation, possibly as a trigger or response to climatic changes. We use neodymium (Nd) isotopic data to reconstruct short high-resolution records of deep-water circulation across the PETM. These records are derived by reductively leaching sediments from seven globally distributed sites and comparing data with published data from fossil fish debris to reconstruct past deep ocean circulation across the PETM. The Nd data for the leachates are interpreted to be consistent with previous studies that have used fish teeth and benthic foraminiferal $\delta^{13}\text{C}$ to constrain regions of convection. There is some evidence from combining Nd isotope and $\delta^{13}\text{C}$ records that the three major ocean basins may not have had substantial exchanges of deep waters. If the isotopic data are interpreted within this framework, then the observed pattern may be explained if the strength of overturning in each basin varied distinctly over the PETM, resulting in differences in deep-water aging gradients between basins. Results are consistent with published interpretations from proxy data and model simulations that suggest modulation of overturning circulation had an important role for global recovery of the ocean–atmosphere system after the PETM.

1 Introduction

The PETM was the warmest time of the past 65 million years (myrs) representing a climatic extreme in which ocean temperatures increased globally by at least 4 °C (Kennett and Stott, 1991; Sluijs et al., 2006; Tripathi and Elderfield, 2004, 2005; Zachos et al., 2001, 2003, 2006) in response to the rapid release in less than 10 000 years (e.g., Farley and Eltgroth, 2003; Murphy et al., 2010; Röhl et al., 2007) of a large amount of carbon from an isotopically light reservoir. Proposed sources for this carbon release

CPD

11, 2557–2583, 2015

Constraints on ocean circulation at the Paleocene–Eocene Thermal Maximum

A. N. Abbott et al.

Title Page

Abstract

Introduction

Conclusions

References

Tables

Figures



Back

Close

Full Screen / Esc

Printer-friendly Version

Interactive Discussion



2005, 2008). Measurements on older sediments ranging from Cenozoic (Martin et al., 2010; Scher and Martin, 2006) to Cretaceous (Martin et al., 2012) in age have shown that sequences from multiple localities can preserve a Nd isotope signal similar to fish teeth and can be used to develop much higher-resolution paleoceanographic records.

2 Materials and methods

2.1 Sample and locality information

Details on the core locations, depths and paleo-depths are given in Table 1. Sources for the carbon isotope data referred to in this study are reported in this table. The age models used to plot all the data (including $\delta^{13}\text{C}$) are shown in Table 2, and are derived from the information given in the publications of the $\delta^{13}\text{C}$ data (Thomas et al., 2003; Nunes and Norris, 2006; Tripathi and Elderfield, 2005). For completeness, we show in Table 2 the core depth-age curve fits that describe the age models for each core, where:

$$\text{Age (Myr)} = m(\text{Core Depth in mbsf}) + b.$$

Several segments are listed if sedimentation rates varied down core (the depth ranges of these segments are listed in Table 2). In all cases, simple linear sedimentation rates were used. These age models were also used to calculate the ages used here for the fish teeth/debris data (Thomas et al., 2003).

2.2 Sample preparation

Freeze-dried sediment samples were obtained from the Integrated Ocean Drilling Program (IODP). One to two grams dry weight of sediment was then rinsed with ultra-high purity (Milli-Q) water, then processed following established sediment leaching protocols (e.g., Bayon et al., 2002; Haley et al., 2008a; Jacobsen and Wasserburg, 1979; Martin

CPD

11, 2557–2583, 2015

Constraints on ocean circulation at the Paleocene–Eocene Thermal Maximum

A. N. Abbott et al.

Title Page

Abstract

Introduction

Conclusions

References

Tables

Figures



Back

Close

Full Screen / Esc

Printer-friendly Version

Interactive Discussion



et al., 2010, 2012; Piotrowski et al., 2008; Scher and Martin, 2006). This procedure basically involves removal of carbonate phases using buffered acetic acid, followed by thorough rinsing with Milli-Q water and then the reduction of early diagenetic metal oxide coatings that carry the bottom water Nd isotope signatures with a dilute buffered hydroxylamine hydrochloric acetic acid solution. This solution leaches the authigenic metal oxide coatings, which are then removed from the sediment and run through standard chromatographic procedures to extract a pure Nd solution for mass spectrometric analyses (AG 50W X12 resin for cation separation followed by di-2-ethylexyl-phosphate resin for rare earth element separation; see Gutjahr et al., 2007 for details). All sediments that could be sampled from the seven sites were analyzed and are presented here.

2.3 Sample analysis

Nd was analyzed on two instruments: a Triton Thermal-Ionization Mass Spectrometer at IFM-GEOMAR, using $^{146}\text{Nd}/^{144}\text{Nd} = 0.7219$ to correct for instrument fractionation, and a Nu Instruments multi-collector inductively coupled mass spectrometer at Oregon State University. Nd isotopes are expressed in ϵ_{Nd} notation, defined as the deviation of measured $^{143}\text{Nd}/^{144}\text{Nd}$ ratios from a bulk Earth value of CHUR (chondritic uniform reservoir) in the 5th decimal place (Thomas et al., 2003). Long-term reproducibility of a Nd standard solution (SPEX source) gave a 2σ error of $0.5 \epsilon_{\text{Nd}}$ units representing the total error of analyses and normalization, exactly as the samples. Analyses of the JNdi standard used for normalization had a lower 2σ error of $0.3 \epsilon_{\text{Nd}}$ units. Nd isotope data are not corrected for decay of samarium given the limited temporal range of the data and the lack of constraints on sample Sm/Nd isotope ratios.

CPD

11, 2557–2583, 2015

Constraints on ocean circulation at the Paleocene–Eocene Thermal Maximum

A. N. Abbott et al.

Title Page

Abstract

Introduction

Conclusions

References

Tables

Figures



Back

Close

Full Screen / Esc

Printer-friendly Version

Interactive Discussion



3 Results and discussion

We have applied a leaching technique (Gutjahr et al., 2007; Haley et al., 2008a, b; Rutberg et al., 2000) that allows the extraction of past bottom water Nd isotope compositions from the Fe-Mn oxide component of marine sediments, expressed as ϵ_{Nd} units (Jacobsen and Wasserburg, 1979) (Table 3). Such data can provide high-resolution records of changes in past deep-water mass mixing and used to interpret changes in circulation (Martin et al., 2010, 2012; Piotrowski et al., 2004, 2005, 2008; Thomas et al., 2014). Below we compare results from leachates to data from fish teeth. We also compare results to carbon isotope data from the same cores. By combining high-resolution ϵ_{Nd} and benthic $\delta^{13}C$ records from the same locations it is possible to elucidate the causes and controls of $\delta^{13}C$ variations in the past deep oceans (Piotrowski et al., 2005). Our new isotopic Nd data are combined with existing $\delta^{13}C$ records and published Nd isotope data from fossil fish teeth of the Atlantic, Indian and Southern Oceans (Thomas et al., 2003), in order to reconstruct global Nd isotope distributions across the PETM at a resolution comparable to the corresponding $\delta^{13}C$ data (Fig. 1).

3.1 Comparison of neodymium isotope data obtained using different archives

Consistent with published results for a number of different sedimentary environments (Martin et al., 2012), we find evidence (Fig. 2) for a general agreement between Nd isotopic data from sediment leaches and fish teeth (Thomas et al., 2003). There appears to be a small, possibly systematic offset at Site 401, and at 690B. This may be the result of higher-order variability at these locations, or the result of a temporal difference between the uptake or the retention of Nd in teeth and the ferromanganese coatings during sedimentation and diagenesis, or a combination of the two. In the first instance, model studies (Lunt et al., 2011; Winguth et al., 2010) have confirmed that locations near the Antarctic continent, such as at Site 690B, were sensitive to changes in climate conditions, and, as such, likely to have varied more substantially during the PETM (Fig. 1).

3.2 Broad patterns in Nd isotope records

The broad patterns in these data support previous studies that have inferred convection occurred in the Southern Ocean, and that convection occurred in both the North and South Pacific (Thomas et al., 2014). The results also are consistent with a relatively insignificant contribution of any Tethyan deep-waters. The ϵ_{Nd} records cover the three major ocean basins (Fig. 1) and reveal distinct and basin-specific changes in deep circulation across the PETM. The ϵ_{Nd} records for eastern North Atlantic Site 401 stabilize at ~ -9.3 during the PETM and then at ~ -8.2 post-PETM, with the trend towards radiogenic values occurring at the end of the PETM. While the fish teeth ϵ_{Nd} record is not a step-function, these are comparable changes to those reported from fish teeth ϵ_{Nd} (Thomas et al., 2003) (Fig. 2). Deep waters at central (eastern) Atlantic Site 1051B, located near the proto-Caribbean, had a more positive ϵ_{Nd} (~ -8) than Site 401 prior to the PETM, but post-PETM ϵ_{Nd} from both sites converged. The record from Site 1051B exhibits similarities to post-PETM data from Site 401, which could reflect more intense mixing within the North Atlantic following the recovery (Fig. 1).

Southern Sites 527 (subtropical South Atlantic) and 690 (Atlantic sector of the Southern Ocean) fluctuated (1 to 1.3 ϵ_{Nd} units) around a mean ϵ_{Nd} of ~ -9 throughout the record, with indications of a switch to in-phase co-variation during and after the PETM, also reflected by the evolution of Site 213 (Fig. 1). Pacific sites 1209B and 1220B were more radiogenic than the other basins (ϵ_{Nd} from -6 to -2). With the exception of one data point (-2.1 ϵ_{Nd} at 55.02 Ma), the western Pacific (Site 1209B) had a remarkably constant ϵ_{Nd} signature of -3.7 pre- and post-PETM. In contrast, the eastern Pacific (Site 1220B) ϵ_{Nd} shows a short excursion from ~ -4 to ~ -5.5 ϵ_{Nd} at the onset of the PETM and remained near unradiogenic endmember values post-PETM ($\epsilon_{\text{Nd}} = -5$) (Fig. 1).

CPD

11, 2557–2583, 2015

Constraints on ocean circulation at the Paleocene–Eocene Thermal Maximum

A. N. Abbott et al.

Title Page

Abstract

Introduction

Conclusions

References

Tables

Figures

◀

▶

◀

▶

Back

Close

Full Screen / Esc

Printer-friendly Version

Interactive Discussion



3.3 A conceptual model to explain the records

The dissimilarities between the ϵ_{Nd} records confirm that the globally similar CIE dominantly reflects a change in source of oceanic carbon (Thomas et al., 2002). This change is not directly from a volcanic or extra-terrestrial source, as these would also be seen in the ϵ_{Nd} records (Cramer and Kent, 2005). However, the ϵ_{Nd} data also clearly indicate that changes in water mass distributions and mixing were associated with the PETM and suggest a fundamentally different circulation system than present must have existed during the PETM. Figure 3 illustrates our reconstruction of the evolution of global deep-water mass exchange during the PETM, based on three distinct deep-water basins that only had restricted water mass exchange between them: the “Southern Ocean,” the North Atlantic and the Pacific.

This conceptual model, based on both $\delta^{13}\text{C}$ and ϵ_{Nd} data, supports changes in areas of convection that are consistent with simulations of the PETM with coupled climate models (Lunt et al., 2012; Thomas et al., 2014) and with a comprehensive climate model (Winguth et al., 2010). It is impossible to interpret from the Nd isotope data alone whether there was reduced or increased overturning associated with carbon release, as these data reflect water mass geometries and not rates of overturning. It is of note that model simulations support a weakening of the meridional overturning circulation with increased greenhouse gases, which might result in a water mass geometry similar to what is reconstructed. However, changes in the exchange between ocean basins will be dependent on several factors, including buoyancy-induced and wind-stress induced changes in overturning, as well as topography. Below we discuss whether there is evidence for changes in ventilation from basinal deep-water aging gradients, and what the nature of topographic barriers would have been to produce the observed patterns in the data.

Constraints on ocean circulation at the Paleocene–Eocene Thermal Maximum

A. N. Abbott et al.

Title Page

Abstract

Introduction

Conclusions

References

Tables

Figures



Back

Close

Full Screen / Esc

Printer-friendly Version

Interactive Discussion



3.3.1 Southern records

An ϵ_{Nd} signature of -9.2 in the “Southern Ocean” most likely reflects an Antarctic margin source, similar to present day Antarctic-sourced intermediate waters (Stichel et al., 2012; Thomas et al., 2003). In agreement with previous inferences from $\delta^{13}\text{C}$ data (Tripathi and Elderfield, 2005; Zeebe and Zachos, 2007), such a deep-water source can readily explain the post-PETM similarity of the ϵ_{Nd} records from both the Southern Atlantic (Site 527) and Indian Ocean (Site 213) with the Atlantic sector of the Southern Ocean (Site 690) (Fig. 3). There are indications that the co-variation of ϵ_{Nd} at Sites 213, 527, and 690 was enhanced during the PETM, which could be consistent with intensification of Southern Ocean-sourced ventilation (Fig. 1a). Previously proposed formation of low-latitude Tethyan deep-water (e.g., Cope and Winguth, 2011; Huber and Sloan, 2001), or slower overturning circulation (Winguth et al., 2010) is unlikely to have generated such range and similarity in evolution of ϵ_{Nd} signatures at these three sites. Furthermore, numerical simulations indicate stronger overturning circulation with multiple deep convection sites provide the best match to the ϵ_{Nd} record (Thomas et al., 2014).

3.3.2 Atlantic Ocean records

The contrast between the Southern Ocean ϵ_{Nd} records and those of the North Atlantic (Fig. 1) indicates that there was little exchange between these basins. The young Mid-Atlantic Ridge (MAR) between Africa and South America most likely represented an efficient barrier for north–south intermediate and deep-water exchange (Bice and Marotzke, 2002). This hypothesis differs from previous interpretations of overturning circulation in the Atlantic (Bice and Marotzke, 2002; Nunes and Norriz, 2006; Thomas et al., 2003), but confirms recent modeling results (Winguth et al., 2010). The differences between the two North Atlantic ϵ_{Nd} records are most simply explained by a weak North Atlantic deep-water overturning cell, with a corresponding higher sensitivity to local changes in Nd inputs or locally variable deep-water masses. Assuming

Constraints on ocean circulation at the Paleocene–Eocene Thermal Maximum

A. N. Abbott et al.

Title Page

Abstract

Introduction

Conclusions

References

Tables

Figures



Back

Close

Full Screen / Esc

Printer-friendly Version

Interactive Discussion



tion at the onset of the PETM. In that case, this Nd isotope shift might simply reflect the progression of a redox front in sediments. Unfortunately, no additional samples are available from site 1220B to further investigate these trends.

However several factors suggest this Nd isotope shift reflects changes in bottom water sourcing and not changes in the position of a sediment redox front. First, a ventilation change in the deep Pacific is in agreement with interpretations of carbon isotope data that support a reversal or large change in deep-water aging gradients between basins (Tripathi and Elderfield, 2005). Secondly, carbonate geochemical data exist which suggest a reversal or dramatic change in deep ocean carbonate saturation gradients between basins, consistent with a circulation change (Zeebe and Zachos, 2007). Thirdly, substantially larger redox changes are observed in PETM sequences from other basins (i.e., the South Atlantic; Chun et al., 2010) that do not exhibit similar corresponding shifts in records of ϵ_{Nd} . Fourthly, similar types of changes are observed during Cretaceous ocean anoxic events (Martin et al., 2012) where there also is no clear-cut evidence for redox fronts driving the sediment leachate ϵ_{Nd} record. Finally, core photographs show that transitions in sediment redox at Site 1220B are not directly coincident with the ϵ_{Nd} change.

Thus we conclude these Nd isotope data are consistent with proxy data (Nunes and Norris, 2006; Tripathi and Elderfield, 2005; Zeebe and Zachos, 2007) and models (Bice and Marotske, 2002; Lunt et al., 2011) and reflect a circulation change at the PETM. These data may record a Pacific circulation “trigger” for carbon release. These data may reflect a change in state of Southern Pacific deep-water source, which some simulations indicate could contribute to hydrate destabilization. Such changes in Southern Ocean water mass characteristics could ultimately have arisen from a gradual forcing such as volcanic outgassing (Kennett and Stott, 1991; Bice and Marotske, 2002; Lunt et al., 2011; Tripathi and Elderfield, 2005).

Constraints on ocean circulation at the Paleocene–Eocene Thermal Maximum

A. N. Abbott et al.

[Title Page](#)[Abstract](#)[Introduction](#)[Conclusions](#)[References](#)[Tables](#)[Figures](#)[Back](#)[Close](#)[Full Screen / Esc](#)[Printer-friendly Version](#)[Interactive Discussion](#)

4 Conclusions

Our study provides new neodymium isotope data from Fe-Mn leachates constraining changes in ocean circulation associated with the PETM. The novelty of these Nd isotope data reflect advances in our ability to extract such data from pelagic sediments, which has opened new avenues of paleoceanographic research. Using Nd isotopes, a proxy independent of carbon cycle processes, we unravel oceanographic changes during the PETM and are able to isolate competing factors controlling the carbon-isotope record during the PETM. In general, we find these data are similar to results from fish teeth (a more widely used proxy), and discuss the combined high-resolution records for seven sites.

The high-resolution combined Nd isotope records provide further evidence for changes in thermohaline circulation associated with the PETM, as previously inferred from basinal carbon isotope gradients (Nunes and Norris, 2006; Tripathi and Elderfield, 2005) and constraints on deep-water carbonate ion concentrations (Zeebe and Zachos, 2007). In addition, these new records provide additional constraints on the timing and the nature of changes in circulation. The records are consistent with variations in bottom water mass mixing in each basin associated with the PETM, with water mass distributions implying intermediate and deep-water circulation changes. We find that changes in deep ocean circulation appear to reflect processes in distinct basins of the Paleocene–Eocene oceans, and as such, may be oversimplified if interpreted in terms of a modern “global conveyor-belt-like” thermohaline circulation. Data from the Pacific exhibit a shift just prior to the carbon isotope excursion, which could indicate that circulation changes preceded the carbon release. Together with modeling results (Bice and Marotzke, 2002; Lunt et al., 2011, 2012; Winguth et al., 2010) and Mg/Ca-based bottom water temperature estimates (Tripathi and Elderfield, 2005), Nd isotope data provide further evidence for thermohaline changes that may have served as a “trigger” of carbon release.

Constraints on ocean circulation at the Paleocene–Eocene Thermal Maximum

A. N. Abbott et al.

Title Page

Abstract

Introduction

Conclusions

References

Tables

Figures



Back

Close

Full Screen / Esc

Printer-friendly Version

Interactive Discussion



The Supplement related to this article is available online at
doi:10.5194/cpd-11-2557-2015-supplement.

Acknowledgements. Samples were provided by the Integrated Ocean Drilling Program. NSF grant 1147407 supported the contributions of A. N. Abbott. A. K. Tripathi was supported by a NERC Fellowship, a Junior Research Fellowship from Magdalene College, and the UCLA Division of Physical Sciences, and thanks Alex Piotrowski for discussing this work and making some pilot measurements. C. Teschner, R. Stumpf and J. Heinze are acknowledged for laboratory support and F. Hauff is thanked for technical support of the mass spectrometer at GEOMAR, Kiel.

References

- Alexander, K., Meissner, K. J., and Bralower, T. J.: Sudden spreading of corrosive bottom water during the Palaeocene–Eocene Thermal Maximum, *Nat. Geosci.*, 8, 458–462, doi:10.1038/NGEO2430, 2015.
- Bayon, G., German, C., Boella, R., Milton, J., Taylor, R., and Nesbitt, R.: An improved method for extracting marine sediment fractions and its application to Sr and Nd isotopic analysis, *Geochim. Cosmochim. Ac.*, 187, 170–199, 2002.
- Bice, K. L. and Marotzke, J.: Could changing ocean circulation have destabilized methane hydrate at the Paleocene/Eocene boundary? *Paleoceanography*, 17, 1018, doi:10.1029/2001pa000678, 2002.
- Bowen, G. J., Koch, P. L., Gingerich, P. D., Norris, R. D., Bains, S., and Corfield, R. M.: Refined isotope stratigraphy across the continental Paleocene–Eocene boundary on Polecat Bench in the northern Bighorn Basin, Paleocene–Eocene stratigraphy and biotic change in the Bighorn and Clarks Fork basins, Wyoming, *University of Michigan Papers on Paleontology*, 33, 73–88, 2001.
- Bowen, G. J., Beerling, D. J., Koch, P. L., Zachos, J. C., and Quattlebaum, T.: A humid climate state during the Palaeocene/Eocene thermal maximum, *Nature*, 432, 495–499, 2004.
- Chun, C. O., Delaney, M. L., and Zachos, J. C.: Paleoredox changes across the Paleocene–Eocene thermal maximum, Walvis Ridge (ODP Sites 1262, 1263, and 1266): evidence from

CPD

11, 2557–2583, 2015

Constraints on ocean circulation at the Paleocene–Eocene Thermal Maximum

A. N. Abbott et al.

Title Page

Abstract

Introduction

Conclusions

References

Tables

Figures



Back

Close

Full Screen / Esc

Printer-friendly Version

Interactive Discussion



Constraints on ocean circulation at the Paleocene–Eocene Thermal Maximum

A. N. Abbott et al.

[Title Page](#)

[Abstract](#)

[Introduction](#)

[Conclusions](#)

[References](#)

[Tables](#)

[Figures](#)



[Back](#)

[Close](#)

[Full Screen / Esc](#)

[Printer-friendly Version](#)

[Interactive Discussion](#)



Mn and U enrichment factors, *Paleoceanography*, 25, PA4202, doi:10.1029/2009PA001861, 2010.

Cope, J. T. and Winguth, A.: On the sensitivity of ocean circulation to arctic freshwater input during the Paleocene/Eocene Thermal Maximum, *Palaeogeogr. Palaeoclimatol.*, 306, 82–94, 2011.

Cramer, B. S. and Kent, D. V.: Bolide summer: the Paleocene/Eocene thermal maximum as a response to an extraterrestrial trigger, *Palaeogeogr. Palaeoclimatol.*, 224, 144–166, doi:10.1016/j.palaeo.2005.03.040, 2005.

Dickens, G. R., O’Niel, J. R., Rea, D. K., and Owen, R. M.: Dissociation of oceanic methane hydrate as a cause of the carbon isotope excursion at the end of the Paleocene, *Paleoceanography*, 10, 965–971, 1995.

Farley, K. A. and Eltgroth, S. F.: An alternative age model for the Paleocene–Eocene thermal maximum using extraterrestrial ^3He , *Earth Planet. Sc. Lett.*, 208, 135–148, 2003.

Frank, M.: Radiogenic isotopes: tracers of part ocean circulation and erosional input, *Rev. Geophys.*, 40, 1001, doi:10.1029/2000RG000094, 2002.

Goldstein, S. L., Hemming, S. R., Heinrich, D. H., and Karl, K. T.: Long-Lived Isotopic Tracers in Oceanography, Paleoceanography, and Ice-Sheet Dynamic, *Treatise on Geochemistry*, edited by: Elderfield, H., 453–489, 2003.

Gutjahr, M., Frank, M., Stirling, C.H., Klemm, V., van de Flierdt, T., and Halliday, A. N.: Reliable extraction of a deepwater trace metal isotope signal from Fe-Mn oxyhydroxide coatings of marine sediments, *Chem. Geol.*, 242, 351–370, doi:10.1016/J.Chemgeo.2007.03.021, 2007.

Haley, B. A., Frank, M., Spielhagen, R. F., and Fietzke, J.: Radiogenic isotope record of Arctic Ocean circulation and weathering inputs of the past 15 million years, *Paleoceanography*, 23, PA1S13, doi:10.1029/2007PA001486, 2008a.

Haley, B. A., Frank, M., Spielhagen, R. F., and Eisenhauer, A.: Influence of brine formation on Arctic Ocean circulation over the past 15 million years, *Nat. Geosci.*, 1, 68–72, doi:10.1038/Ngeo.2007.5, 2008b.

Higgins, J. A. and Schrag, D. P.: Beyond methane: towards a theory for the Paleocene–Eocene Thermal Maximum, *Earth Planet. Sc. Lett.*, 245, 523–537, doi:10.1016/j.epsl.2006.03.009, 2006.

Huber, M. and Sloan, L. C.: Heat transport, deep waters, and thermal gradients: coupled simulation of an Eocene Greenhouse Climate, *Geophys. Res. Lett.*, 28, 3481–3484, 2001.

Constraints on ocean circulation at the Paleocene–Eocene Thermal Maximum

A. N. Abbott et al.

[Title Page](#)

[Abstract](#)

[Introduction](#)

[Conclusions](#)

[References](#)

[Tables](#)

[Figures](#)

[◀](#)

[▶](#)

[◀](#)

[▶](#)

[Back](#)

[Close](#)

[Full Screen / Esc](#)

[Printer-friendly Version](#)

[Interactive Discussion](#)



- Jacobsen, S. B. and Wasserburg, G. J.: Mean age of mantle and crustal reservoirs, *J. Geophys. Res.*, 85, 7411–7427, 1979.
- Kennett, J. P. and Stott, L. D.: Abrupt deep-sea warming, palaeoceanographic changes and benthic extinctions at the end of the Palaeocene, *Nature*, 353, 225–229, 1991.
- 5 Koch, P. L., Zachos, J. C., and Gingerich, P. D.: Correlation between isotope records in marine and continental carbon reservoirs near the Paleocene Eocene boundary, *Nature*, 358, 319–322, 1992.
- Kurtz, A. C., Kump, L. R., Arthur, M. A., Zachos, J. C., and Paytan, A.: Early Cenozoic decoupling of the global carbon and sulfur cycles, *Paleoceanography*, 18, 1090, doi:10.1029/2003pa000908, 2003.
- 10 Lunt, D. J., Ridgwell, A., Sluijs, A., Zachos, J., Hunter, S., and Haywood, A.: A model for orbital pacing of methane hydrate destabilization during the Palaeogene, *Nat. Geosci.*, 4, 775–778, doi:10.1038/Ngeo1266, 2011.
- Lunt, D. J., Dunkley Jones, T., Heinemann, M., Huber, M., LeGrande, A., Winguth, A., Loptson, C., Marotzke, J., Roberts, C. D., Tindall, J., Valdes, P., and Winguth, C.: A model–data comparison for a multi-model ensemble of early Eocene atmosphere–ocean simulations: EoMIP, *Clim. Past*, 8, 1717–1736, doi:10.5194/cp-8-1717-2012, 2012.
- 15 Martin, E. E., Blair, S. W., Kamenov, G. D., Scher, H. D., Bourbon, E., Basak, C., and Newkirk, D. N.: Extraction of Nd isotopes from bulk deep sea sediments for paleoceanographic studies on Cenozoic time scales, *Chem. Geol.*, 269, 414–431, 2010.
- Martin, E. E., MacLeod, K. G., Berrocoso, A. J., and Bourbon, E.: Water mass circulation on Demerara Rise during the Late Cretaceous based on Nd isotopes, *Earth Planet. Sc. Lett.*, 327–328, 111–120, 2012.
- 20 McCarren, H., Thomas, E., Hasegawa, T., Rohl, U., and Zachos, J. C.: Depth dependency of the Paleocene–Eocene carbon isotope excursion: paired benthic and terrestrial biomarker records (Ocean Drilling Program Leg 208, Walvis Ridge), *Geochem. Geophys. Geosy.*, 9, Q10008, doi:10.1029/2008gc002116, 2008.
- McInerney, F. A. and Wing, S. L. The Paleocene–Eocene Thermal Maximum: a perturbation of carbon cycle, climate, and biosphere with implications for the future, *Annu. Rev. Earth Pl. Sc.*, 39, 489–516, 2011.
- 30 Murphy, B. H., Farley, K. A., and Zachos, J. C.: An extraterrestrial ^3He -based timescale for the Paleocene–Eocene thermal maximum (PETM) from Walvis Ridge, IODP Site 1266, *Geochim. Cosmochim. Ac.*, 74, 5098–5108, 2010.

Constraints on ocean circulation at the Paleocene–Eocene Thermal Maximum

A. N. Abbott et al.

Title Page

Abstract

Introduction

Conclusions

References

Tables

Figures



Back

Close

Full Screen / Esc

Printer-friendly Version

Interactive Discussion



- Nunes, F. and Norris, R. D.: Abrupt reversal in ocean overturning during the Palaeocene/Eocene warm period, *Nature*, 439, 60–63, doi:10.1038/Nature04386, 2006.
- Pagani, M., Pedentchouk, N., Huber, M., Sluijs, A., Schouten, S., Brinkhuis, H., Sinninghe-Damste, J., and Dickens, G. R.: Arctic hydrology during global warming at the Palaeocene/Eocene thermal maximum, *Nature*, 442, 671–675, 2006.
- Paytan, A., Averyt, K., Faul, K., Gray, E., and Thomas, E.: Barite accumulation, ocean productivity, and Sr/Ba in barite across the Paleocene–Eocene Thermal Maximum, *Geology*, 35, 1139–1142, doi:10.1130/G24162A.1, 2007.
- Piotrowski, A. M., Goldstein, S. L., Hemming, S. R., and Fairbanks, R. G.: Intensification and variability of ocean thermohaline circulation through the last deglaciation, *Earth Planet. Sc. Lett.*, 225, 205–220, 2004.
- Piotrowski, A. M., Goldstein, S. L., Hemming, S. R., and Fairbanks, R. G.: Temporal relationships of carbon cycling and ocean circulation at glacial boundaries, *Science*, 307, 1933–1938, doi:10.1126/Science.1104883, 2005.
- Piotrowski, A. M., Goldstein, S. L., Hemming, S., Fairbanks, R. G., and Zylberberg, D. R.: Oscillating glacial northern and southern deep water formation from combined neodymium and carbon isotopes, *Earth Planet. Sc. Lett.*, 272, 394–405, 2008.
- Röhl, U., Westerhold, T., Bralower, T. J., and Zachos, J. C.: On the duration of the Paleocene–Eocene thermal maximum (PETM), *Geochem. Geophys. Geosy.*, 8, Q12002, doi:10.1029/2007GC001784, 2007.
- Rutberg, R. L., Hemming, S. R., and Goldstein, S. L.: Reduced North Atlantic Deep Water flux to the glacial Southern Ocean inferred from neodymium isotope ratios, *Nature*, 405, 935–938, 2000.
- Scher, H. D. and Martin, E. E.: Timing and climatic consequences of the opening of Drake Passage, *Science*, 312, 428–430, doi:10.1126/Science.1120044, 2006.
- Sluijs, A., Schouten, S., Pagani, M., Woltering, M., Brinkhuis, H., Damsté, J. S. S., Dickens, J. and Moran, K.: Subtropical Arctic Ocean temperatures during the Palaeocene/Eocene thermal maximum, *Nature*, 441, 610–613, 2006.
- Sluijs, A., Brinkhuis, H., Schouten, S., Bohaty, S. M., John, C. M., Zachos, J. C., Reichert, G.-J., Sinninghe Damsté, J. S., Crouch, E. M., and Dickens, G. R.: Environmental precursors to rapid light carbon injection at the Palaeocene/Eocene boundary, *Nature*, 450, 1218–1221, 2007.

Constraints on ocean circulation at the Paleocene–Eocene Thermal Maximum

A. N. Abbott et al.

Title Page

Abstract

Introduction

Conclusions

References

Tables

Figures



Back

Close

Full Screen / Esc

Printer-friendly Version

Interactive Discussion



Stichel, T., Frank, M., Rickli, J., and Haley, B. A.: The hafnium and neodymium isotope composition of seawater in the Atlantic sector of the Southern Ocean, *Earth Planet. Sc. Lett.*, 317–318, 282–294, 2012.

Storey, M., Duncan, R. A., and Swisher, C. C.: Paleocene–Eocene thermal maximum and the opening of the northeast Atlantic, *Science*, 316, 587–589, doi:10.1126/Science.1135274, 2007.

Svensen, H., Planke, S., Malthé-Sørensen, A., Jamtveit, B., Myklebust, R., Eidem, T. R., and Rey, S. S.: Release of methane from a volcanic basin as a mechanism for initial Eocene global warming, *Nature*, 429, 542–545, doi:10.1038/Nature02566, 2004.

Thomas, D. J.: Evidence for deep-water production in the North Pacific Ocean during the early Cenozoic warm interval, *Nature*, 430, 65–68, doi:10.1038/nature02639, 2004.

Thomas, D. J., Zachos, J. C., Bralower, T. J., Thomas, E., and Bohaty, S.: Warming the fuel for the fire: Evidence for the thermal dissociation of methane hydrate during the Paleocene–Eocene thermal maximum, *Geology*, 30, 1067–1070, 2002.

Thomas, D. J., Bralower, T. J., and Jones, C. E.: Neodymium isotopic reconstruction of late Paleocene–early Eocene thermohaline circulation, *Earth Planet. Sc. Lett.*, 209, 309–322, doi:10.1016/S0012-821x(03)00096-7, 2003.

Thomas, D. J., Lyle, M., Moore, T. C., and Rea, D. K.: Paleogene deepwater mass composition of the tropical Pacific and implications for thermohaline circulation in a greenhouse world, *Geochem. Geophys. Geosy.*, 9, Q02002, doi:10.1029/2007gc001748, 2008.

Thomas, D. J., Korty, R., Huber, M., Schubert, J. A., Haines, B.: Nd isotopic structure of the Pacific Ocean 70–30 Ma and numerical evidence for vigorous ocean circulation and ocean heat transport in a greenhouse world, *Paleoceanography*, 29, 454–469, doi:10.1002/2013PA002535, 2014.

Tripathi, A. K. and Elderfield, H.: Abrupt hydrographic changes in the equatorial Pacific and subtropical Atlantic from foraminiferal Mg/Ca indicate greenhouse origin for the thermal maximum at the Paleocene–Eocene Boundary, *Geochem. Geophys. Geosy.*, 5, Q02006, doi:10.1029/2003GC000631, 2004.

Tripathi, A. and Elderfield, H.: Deep-sea temperature and circulation changes at the Paleocene–Eocene thermal maximum, *Science*, 308, 1894–1898, doi:10.1126/Science.1109202, 2005.

Winguth, A., Shellito, C., Shields, C., and Winguth, C.: Climate response at the Paleocene–Eocene Thermal Maximum to greenhouse gas forcing – a model study with CCSM3, *J. Climatol.*, 23, 2562–2584, doi:10.1175/2009jcli3113.1, 2010.

Constraints on ocean circulation at the Paleocene–Eocene Thermal Maximum

A. N. Abbott et al.

[Title Page](#)[Abstract](#)[Introduction](#)[Conclusions](#)[References](#)[Tables](#)[Figures](#)[Back](#)[Close](#)[Full Screen / Esc](#)[Printer-friendly Version](#)[Interactive Discussion](#)

Zachos, J., Pagani, M., Sloan, L., Thomas, E., and Billups, K.: Trends, rhythms, and aberrations in global climate 65 Ma to present, *Science*, 292, 686–693, 2001.

Zachos, J. C., Wara, M. W., Bohaty, S., Delaney, M. L., Petrizzo, M. R., Brill, A., Bralower, T. J., and Premoli-Silva, I.: A transient rise in tropical sea surface temperature during the Paleocene–Eocene Thermal Maximum, *Science*, 302, 1551–1554, doi:10.1126/Science.1090110, 2003.

Zachos, J. C., Schouten, S., Bohaty, S., Quattlebaum, T., Sluijs, A., Brinkhuis, H., Gibbs, S. and Bralower, T. J.: Extreme warming of mid-latitude coastal ocean during the Paleocene–Eocene Thermal Maximum: inferences from TEX86 and isotope data, *Geology*, 34, 737–740, 2006.

Zeebe, R. E. and Zachos, J. C.: Reversed deep-sea carbonate ion basin gradient during Paleocene–Eocene thermal maximum, *Paleoceanography*, 22, 3201, doi:10.1029/2006PA001395, 2007.

Zeebe, R. E., Zachos, J. C., and Dickens, G. R.: Carbon dioxide forcing alone insufficient to explain Palaeocene–Eocene Thermal Maximum warming, *Nat. Geosci.*, 2, 576–580, doi:10.1038/ngeo578, 2009.

Constraints on ocean circulation at the Paleocene–Eocene Thermal Maximum

A. N. Abbott et al.

[Title Page](#)

[Abstract](#)

[Introduction](#)

[Conclusions](#)

[References](#)

[Tables](#)

[Figures](#)

[⏪](#)

[⏩](#)

[◀](#)

[▶](#)

[Back](#)

[Close](#)

[Full Screen / Esc](#)

[Printer-friendly Version](#)

[Interactive Discussion](#)



Table 2. Age Models.

Core	Age model segment	Core depth (MBSF)		Curve definition	
		start	end	<i>m</i>	<i>b</i>
1209B	a	210.72	211.24	0.3539	−19.317
	b	211.26	211.40	2.5000	−472.660
213	a	145.13	147.35	0.2541	+17.727
	b	147.41	147.64	0.1193	+37.590
401	a	198.54	201.97	0.1640	+22.054
	b	202.02	202.98	0.0656	+41.922
1220B	a	197.55	199.20	0.4009	−24.697
	b	199.25	199.93	0.0955	+36.159
527	a	199.63	200.71	0.2027	+14.491
	b	200.89	202.76	0.0700	+41.129
690B	a	162.80	170.69	0.0646	+44.199
	b	170.71	170.76	0.0453	+47.528
	c	170.84	172.49	0.1923	+22.416
	d	172.95	179.80	0.1167	+35.192
1051B	a	510.17	512.35	0.1164	−4.439
	b	512.40	513.80	0.2100	−52.412

Table 3. Summary of neodymium isotope data.

Hole	Core Section	Depth Interval (cm)		ϵ_{Nd}	age (Ma)
		upper	lower		
1220B	20X-1	65	67	-5.70	54.70
1220B	20X-1	85	87	-5.80	54.78
1220B	20X-1	110	112	-5.50	54.88
1220B	20X-1	135	137	-5.70	54.98
1220B	20X-1	145	147	-5.60	55.02
1220B	20x-2	5	7	-5.90	55.06
1220B	20x-2	10	12	-5.40	55.08
1220B	20x-2	15	17	-5.60	55.10
1220B	20x-2	20	22	-4.60	55.12
1220B	20x-2	25	27	-4.40	55.14
1220B	20x-2	30	32	-4.50	55.16
1220B	20x-2	35	37	-4.10	55.18
1220B	20x-2	40	42	-4.00	55.19
1220B	20x-2	80	82	-5.40	55.22
1220B	20x-2	90	92	-5.00	55.23
1220B	20x-2	93	94	-6.00	55.24
1220B	20x-CCW	5	6	-4.31	55.24
1220B	20x-CCW	6	7	-3.41	55.25
1209B	22H-1	12	14	-2.10	55.02
1209B	22H-1	39	40	-3.68	55.10
1209B	22H-1	47	48	-3.71	55.13
1209B	22H-1	48	49	-3.69	55.14
1209B	22R-1	84	86	-3.50	55.28
1209B	22R-1	108	110	-3.70	55.37
1209B	22R-1	120	122	-3.50	55.41
1209B	22R-1	132	134	-4.00	55.45
1209B	22R-1	148	150	-3.70	55.85
0690B	18H-5	36	37	-9.70	54.77
0690B	18H-6	30	31	-8.40	54.84
0690B	18H-6	110	111	-9.70	54.91
0690B	19H-1	30	31	-8.80	55.00
0690B	19H-1	65	66	-9.10	55.03
0690B	19H-1	137	138	-8.70	55.07
0690B	19H-2	47	48	-9.90	55.11
0690B	19H-2	109	110	-9.90	55.15
0690B	19H-3	69	71	-8.30	55.21
0690B	19H-4	66	67	-9.30	55.31
0690B	19H-5	6	7	-8.80	55.36
0690B	19H-5	65	66	-9.10	55.44
0690B	19H-5	106	107	-9.20	55.48
0690B	20H-1	3	4	-9.63	55.53
0690B	20H-1	140	141	-9.84	55.80
0690B	20H-2	111	112	-9.20	56.17

Constraints on ocean circulation at the Paleocene–Eocene Thermal Maximum

A. N. Abbott et al.

Title Page

Abstract Introduction

Conclusions References

Tables Figures

◀ ▶

◀ ▶

Back Close

Full Screen / Esc

Printer-friendly Version

Interactive Discussion



Table 3. Continued.

Hole	Core Section	Depth Interval (cm)		ϵ_{Nd}	age (Ma)
		upper	lower		
527	24R-1	11	12	-8.27	54.85
527	24R-1	31	32	-9.98	54.89
527	24R-1	53	54	-7.95	54.94
527	24R-1	81	82	-9.26	54.99
527	24R-1	100	102	-8.50	55.00
527	24R-1	140	142	-9.60	55.12
527	24R-2	11	12	-8.96	55.13
527	24R-2	41	42	-9.20	55.15
527	24R-2	87	88	-9.02	55.16
527	24R-2	24	27	-9.30	55.18
527	24R-2	30	33	-8.90	55.20
527	24R-2	47	48	-8.40	55.20
527	24R-3	59	60	-9.29	55.29
527	24R-3	81	82	-9.85	55.30
527	24R-3	121	122	-9.18	55.33
527	24R-4	10	11	-8.89	55.40
527	24R-4	40	41	-9.12	55.42
527	24R-4	80	81	-9.08	55.40
213	16-3	48	49	-8.60	54.69
213	16-4	8	9	-8.40	54.97
213	16-4	49	50	-9.00	55.08
213	16-4	58	59	-9.30	55.10
213	16-4	90	91	-9.50	55.17
213	16-4	99	100	-9.50	55.19
1051B	59X-2	110	111	-8.23	54.50
1051B	59X-2	139	140	-8.41	54.60
1051B	59X-3	26	27	-8.26	54.76
1051B	59X-3	46	47	-8.65	54.80
1051B	59X-3	67	68	-8.81	54.90
1051B	59X-3	87	88	-8.75	54.94
1051B	59X-3	120	120	-8.70	54.97
1051B	60X-1	65	65	-9.00	55.09
1051B	60X-1	119	120	-9.00	55.15
1051B	60X-1	145	145	-8.30	55.18
1051B	60X-2	56	56	-8.00	55.31
1051B	60X-2	64	66	-7.40	55.33
1051B	60X-2	74	75	-8.00	55.35
1051B	60X-2	84	85	-8.05	55.37
1051B	60X-2	93	94	-8.20	55.39
1051B	60X-2	109	110	-7.89	55.42
1051B	60X-2	118	119	-7.79	55.44
1051B	60X-2	142	143	-7.93	55.52

Constraints on ocean circulation at the Paleocene–Eocene Thermal Maximum

A. N. Abbott et al.

[Title Page](#)

[Abstract](#) [Introduction](#)

[Conclusions](#) [References](#)

[Tables](#) [Figures](#)

[◀](#) [▶](#)

[◀](#) [▶](#)

[Back](#) [Close](#)

[Full Screen / Esc](#)

[Printer-friendly Version](#)

[Interactive Discussion](#)



Constraints on ocean circulation at the Paleocene–Eocene Thermal Maximum

A. N. Abbott et al.

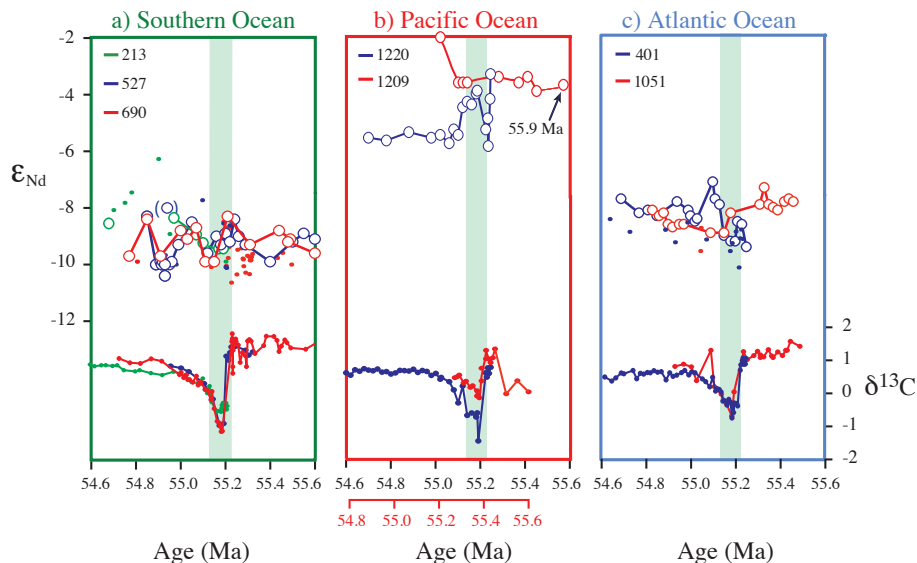


Figure 1. Nd and C isotope data (ϵ_{Nd} and $\delta^{13}C$) across the PETM from the Southern Ocean (a), Pacific Ocean (b), and Atlantic Basins (c). The sediment leach ϵ_{Nd} are shown with circles and solid lines; the fish teeth/debris ϵ_{Nd} from Thomas et al. (2003) are shown as dots. All data are presented on directly comparable scales for both ϵ_{Nd} and $\delta^{13}C$. The sample ages are based on the $\delta^{13}C$ age models. In (b) the age model of Site 1209B has been slightly adjusted (second x axis) such that the $\delta^{13}C$ excursion coincides with the age of the PETM in the other cores. The shaded vertical bar indicates the timing of the PETM as defined by the CIE in the cores.

Title Page

Abstract

Introduction

Conclusions

References

Tables

Figures

◀

▶

◀

▶

Back

Close

Full Screen / Esc

Printer-friendly Version

Interactive Discussion



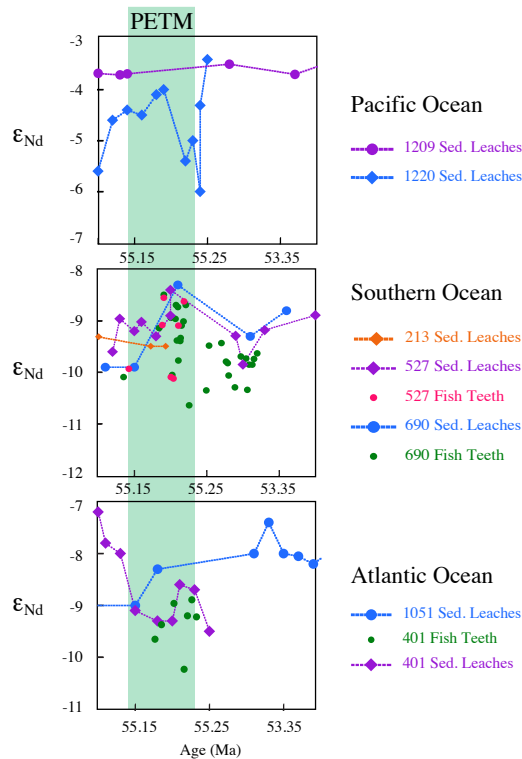


Figure 2. Sediment leach ϵ_{Nd} and available fish teeth ϵ_{Nd} data from 55.1 to 55.4 Ma for all three ocean basins. Sediment ϵ_{Nd} values are connected with a dotted line and fish teeth data are represented by unconnected dots. The green shaded area represents the PETM as marked by the carbon isotope excursion from each core. These data sources are generally consistent, although higher-order differences, likely intrinsic to the natures of the archival sources, are present.

Constraints on ocean circulation at the Paleocene–Eocene Thermal Maximum

A. N. Abbott et al.

Title Page

Abstract

Introduction

Conclusions

References

Tables

Figures

◀

▶

◀

▶

Back

Close

Full Screen / Esc

Printer-friendly Version

Interactive Discussion



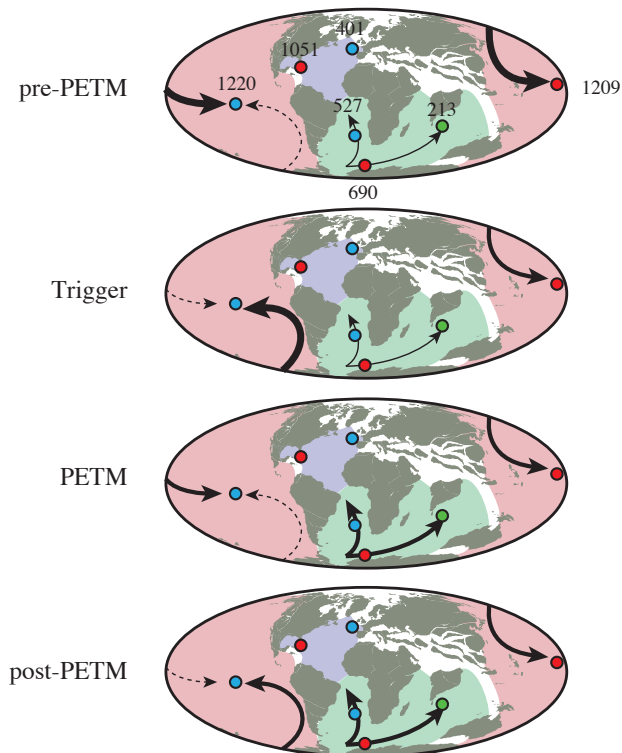


Figure 3. A conceptual model of the intermediate/deep-water mixing changes across the PETM as inferred from ϵ_{Nd} records of intermediate/deep-water mass geometries. Arrow boldness reflects overturning circulation that could produce water mass geometries. Dashed arrows represent weak overturning. The arrow directions reflect our interpretation of the general direction of flow, and are not meant to be viewed as precise flow-paths. The paleogeographic distribution of the continents is from Ocean Drilling Stratigraphic Network (ODSN).

Constraints on ocean circulation at the Paleocene–Eocene Thermal Maximum

A. N. Abbott et al.

Title Page

Abstract

Introduction

Conclusions

References

Tables

Figures

◀

▶

◀

▶

Back

Close

Full Screen / Esc

Printer-friendly Version

Interactive Discussion

